J. MACROMOL. SCI.—PHYS., B39(2), 257–277 (2000)

Application of the Avrami, Tobin, Malkin, and Simultaneous Avrami Macrokinetic Models to Isothermal Crystallization of Syndiotactic Polypropylenes

PITT SUPAPHOL* and JOSEPH E. SPRUIELL†
Center for Materials Processing and
Department of Materials Science and Engineering
University of Tennessee
Knoxville, Tennessee

ABSTRACT

Various macrokinetic models (the Avrami, Tobin, Malkin, and simultaneous Avrami models) were applied to describe the primary crystallization of syndiotactic polypropylene (sPP) under isothermal conditions. Analysis of the experimental data was carried out using a direct-fitting method such that the experimental data were fitted directly to each macrokinetic model using a nonlinear multivariable regression program. Comparison of the kinetics parameters obtained from the program to those obtained from the traditional analytical procedure suggested that applicability and reliability of the direct-fitting method are satisfactory. Prediction of the time-dependent relative evolution of crystallinity at other crystallization temperatures was demonstrated based on the bulk kinetics parameters obtained from the analysis.

Key Words. Avrami analysis, Isothermal crystallization, Macrokinetic model, Malkin analysis, Syndiotactic polypropylene, Tobin analysis.

*Current address: Petroleum and Petrochemical College, Chulalongkorn University, Soi Chulalongkorn 12, Phyathai Road, Pathumwan, Bangkok 10330, Thailand.
†To whom correspondence should be addressed at: 434 Dougherty Engineering Building, Knoxville, TN 37996-2000. E-mail: spruiell@utk.edu

INTRODUCTION

The overall crystallization process in semicrystalline polymers can be divided into two main processes: primary crystallization and secondary crystallization. The primary crystallization process is the macroscopic development of crystallinity as a result of two consecutive microscopic mechanisms: primary nucleation and secondary nucleation (i.e., subsequent crystal growth). The secondary crystallization process is mainly concerned with the crystallization of interfibrillar melt, which was rejected and trapped between the fibrillar structure formed during the growth of crystalline aggregates (e.g., axialites, spherulites, etc.) [1–3]. It should be noted that, if the crystallization time becomes very long, other types of secondary crystallization (i.e., crystal perfection and crystal thickening) may become significant enough to increase the ultimate absolute crystallinity.

For the purpose of describing the macroscopic evolution of crystallinity under quiescent isothermal conditions, a number of mathematical models [4–13] have been proposed, based primarily on the notion of primary nucleation and subsequent crystal growth microscopic mechanisms, over the past 60 years. Even though the contributions from Kolmogoroff [4], Johnson and Mehl [5], Avrami [6–8], and Evans [9] are essentially similar, it is the work of Avrami that has received the most attention. Therefore, these contributions are frequently referred to as the "Avrami equation." Based on different approaches, Tobin [10–12] and Malkin et al. [13] arrived at different mathematical models, which are also different from the Avrami model. Consequently, the quiescent crystallization data of semicrystalline polymers at a constant temperature can be described mathematically by these three distinct models.

Unlike the Avrami model, use of the Tobin and Malkin models to analyze the isothermal crystallization data of semicrystalline polymers is scarce. Critical descriptive comparisons between the Avrami and Tobin models were performed on the isothermal crystallization data of poly(ethylene terephthalate) (PET), poly(phenylene sulfide) (PPS) [14], medium-density polyethylene (MDPE), and poly(oxymethylene) (POM) [15]. On the other hand, critical descriptive comparisons between the Avrami and Malkin models were performed on isothermal crystallization data of polyethylene (PE), isotactic polypropylene (iPP), PET, poly(propylene oxide) (PPO), and polyurethane (PU) [13].

To the best of our knowledge, critical analysis of the experimental data, and hence the descriptive comparison of the results, using all three models has not been described in the literature thus far. Therefore, in the present contribution, all three macrokinetic models are used to analyze the isothermal crystallization data of syndiotactic polypropylene (sPP). The experimental data are fitted to each respective model using a nonlinear multivariable regression program. The goodness of the fit suggests the applicability of the model in describing the isothermal crystallization data of sPP.

THEORY

The overall crystallization kinetics of polymers are usually analyzed using the Avrami equation [4–9]. When applied for use with differential scanning calorimetry (DSC), it is assumed that the differential area under the crystallization curve with time corresponds to the dynamic changes in the conversion of mass from the melt phase to the solid phase. If χ_∞ and χ_t are the maximum crystallinity obtained for particular crystallization condition and the dynamic crystallinity at arbitrary time t for the same crystallization condition, respectively, then the governing Avrami equation can be written as

MARCEL DEKKER, INC.
270 Madison Avenue, New York, New York 10016

$$\chi_t/\chi_\infty = \theta(t) = 1 - \exp(-k_a t^{n_a}) \tag{1}$$

where $\theta(t)$ denotes the relative crystallinity as a function of time, k_a is the Avrami crystallization rate constant, and n_a is the Avrami exponent of time. Both k_a and n_a are constants typical of a given crystalline morphology and type of nucleation for a particular crystallization condition [16]. It should be noted that, according to the original assumptions of the theory, the value of n_a should be integral, ranging from 1 to 4.

In the study of isothermal crystallization using DSC, the rate of evolution of the heat of crystallization as a function of time and the relative extent of crystallization $\theta(t)$ are related to one another according to the following equation:

$$\theta(t) = \frac{\int_0^t \left(\frac{dH_c}{dt}\right) dt}{\Delta H_c} \tag{2}$$

where t represents an arbitrary time during the course of isothermal crystallization process, dH_c is the enthalpy of crystallization released during an infinitesimal time interval dt, and ΔH_c is the overall enthalpy of crystallization for a specific crystallization temperature T_c.

An important remark that has been made on the Avrami model is that the equation is only appropriate for the early stages of crystallization. Aiming at improving the Avrami model, Tobin [10–12] proposed a different expression describing phase transformation kinetics with growth site impingement. The original theory was written in a form of nonlinear Volterra integral equation, of which zeroth-order solution is given by

$$\theta(t) = \frac{k_t t^{n_t}}{1 + k_t t^{n_t}} \tag{3}$$

where $\theta(t)$ is the relative crystallinity as a function of time, k_t is the Tobin crystallization rate constant, and n_t is the Tobin exponent. Based on this proposition, the Tobin exponent of time n_t needs not be integral [11,12], and it is governed directly by different types of nucleation and growth mechanisms. It is worth noting that a similar expression was considered by Rabesiaka and Kovacs [17], and it was found to give a good fit to their dilatometric data of linear PE for $\theta(t)$ up to 0.9.

Derived based on the notion that the overall crystallization rate equals the summation of the rate at which the degree of crystallinity varies as a result of emergence of the primary nuclei and the rate of variation in the degree of crystallinity as a result of crystal growth, Malkin et al. [13] proposed a totally different form of a macrokinetic equation:

$$\theta(t) = 1 - \frac{C_0 + 1}{C_0 + \exp(C_1 t)} \tag{4}$$

where $\theta(t)$ is the relative crystallinity as a function of time. C_0 relates directly to the ratio of the linear growth rate G to the nucleation rate N (i.e., $C_0 \propto G/N$), and C_1 relates directly to the overall crystallization rate (i.e., $C_1 = a \cdot N + b \cdot G$, where a and b are specific constants). Apparently, both C_0 and C_1 are temperature-dependent constants.

Analyses of the experimental data based on the Avrami and Tobin approaches are straightforward. The Avrami kinetics parameters k_a and n_a can be extracted from the least-square line fitted to the double logarithmic plot of $\ln[-\ln(1 - \theta(t))]$ versus $\ln(t)$; k_a is the antilogarithmic value of the y-intercept, and n_a is the slope of the least-square line.

MARCEL DEKKER, INC.
270 Madison Avenue, New York, New York 10016

Similarly, the Tobin crystallization kinetics parameters k_t and n_t can be extracted by drawing a least-square line fitted to the double logarithmic plot of $\ln[\theta(t)/(1-\theta(t))]$ versus $\ln(t)$; here, k_t is the antilogarithmic value of the y-intercept, and n_t is the slope. It should be noted that, in both cases, the kinetics parameters are calculated from the least-square line drawn through the bulk of the data in the range $0.10 < \theta(t) < 0.80$. In the case of the Malkin approach, the authors proposed a shortcut method of determining their kinetics parameters C_0 and C_1 from those obtained from the Avrami analysis [13]:

$$C_0 = 4^{n_a} - 4 \tag{5}$$

and

$$C_1 = \ln(4^{n_a} - 2)\left(\frac{k_a}{\ln(2)}\right)^{1/n_a} \tag{6}$$

In light of this being the computational age, a computer seems to be an indispensable tool in almost every aspect of our lives. Instead of analyzing the experimental data using the traditional procedure mentioned earlier, we use a nonlinear multivariable regression program to fit the experimental data directly to the three aforementioned macrokinetic models. The goodness of the fit is described by the chi-square parameter χ^2 [18], in which the lower the value, the better the fit. In addition, the corresponding kinetics parameters required by each model are automatically provided by the program once the best fit is determined. The applicability and reliability of the program were verified by comparing the Avrami kinetics parameters obtained based on the traditional procedure with those provided by the program.

EXPERIMENTAL

Materials

The two sPP samples used in this study were supplied in pellet form by Fina Oil and Chemical Company (La Porte, TX). Molecular characterization of these materials was kindly performed by Dr. Roger A. Phillips and his coworkers at Montell USA, Incorporated, in Elkton, Maryland. The results are listed in Table 1. It should be noted that sPP 3 has a bimodal molecular weight distribution, which results in an unusually high degree of polydispersity.

TABLE 1

Characterization Data of As-Received Syndiotactic Polypropylene Samples

Sample	Intrinsic viscosity, $dL \cdot g^{-1}$	M_n	M_w	M_z	M_w/M_n	Racemic pentads, %*rrrr*	Racemic triads, %*rr*	Racemic dyads, %*r*	Ethylene content, % by wt
sPP 1	1.61	76,200	165,000	290,000	2.2	77.1	87.3	91.4	1.3
sPP 3	1.32	37,300	133,000	308,000	3.6	74.6	83.7	88.3	0.5

Technique and Sample Preparation

A Perkin-Elmer Series 7 differential scanning calorimeter (DSC7) was used to follow the isothermal crystallization in this study. The DSC7 equipped with an internal liquid nitrogen cooling unit dependably provided a cooling rate up to 200°C·min^{-1}. Temperature calibration was performed using indium as a standard; it has the following thermal properties: $T_m^o = 156.6$°C and $\Delta H_f^o = 28.5$ J·g^{-1}. The consistency of the temperature calibration was checked every other run to ensure reliability of the data obtained. To make certain that thermal lag between the polymeric sample and the DSC sensors was kept to a minimum, each sample holder was loaded with a single disk weighing around 4.9 ± 0.3 mg. A hole puncher was used to cut the disk from a film. The film was prepared by melt pressing virgin pellets, placed between a pair of Kapton films, which in turn were sandwiched between a pair of stainless steel platens, in a Wabash compression-molding machine at 190°C under a pressure of 67 kpsi. After 10 min holding time, the film, approximately 280 μm thick, was taken out and immediately submerged in an ice-water bath while it was still between the two steel platens. By this treatment, we assume that previous thermal and mechanical histories were essentially erased, providing a controlled condition for the film.

Methods

The experiment started by heating the sample from −40°C at a scanning rate of 80°C·min^{-1} to 190°C and holding it there for 5 min before quenching at a cooling rate of 200°C·min^{-1} to a desired isothermal crystallization temperature T_c. It should be noted that melting of a sample at 190°C for at least 5 min is necessary and ample to erase previous thermal history [19] (i.e., complete melting). It was assumed that the crystallization finished when the exothermic trace converged to a horizontal baseline. The crystallization exotherms were then recorded for further analysis.

RESULTS AND DISCUSSION

Isothermal Crystallization of Syndiotactic Polypropylene from the Melt

By assuming that the evolution of the crystallinity is linearly proportional to the evolution of heat released during isothermal crystallization in the DSC, the relative evolution of the crystallinity as a function of time $\theta(t)$ can thus be calculated by integration of the crystallization exothermic traces according to Eq. 2. The relative crystallinity as a function of time $\theta(t)$ of both sPP samples are plotted in Fig. 1 for four different crystallization temperatures T_c ranging from 75°C to 90°C. Clearly, the time to reach the ultimate crystallinity increases with increasing crystallization temperature. An important kinetics parameter that can be taken directly from the curve of $\theta(t)$ versus time t is the half-time of crystallization $t_{0.5}$, which is defined as the time taken from the onset of the crystallization until 50% completion. A summary of the crystallization half-time $t_{0.5}$ values for both sPP samples is listed in Table 2, whereas the plots of $t_{0.5}$ versus T_c (including the plots of its reciprocal value $t_{0.5}^{-1}$ versus T_c) are shown in Fig. 2.

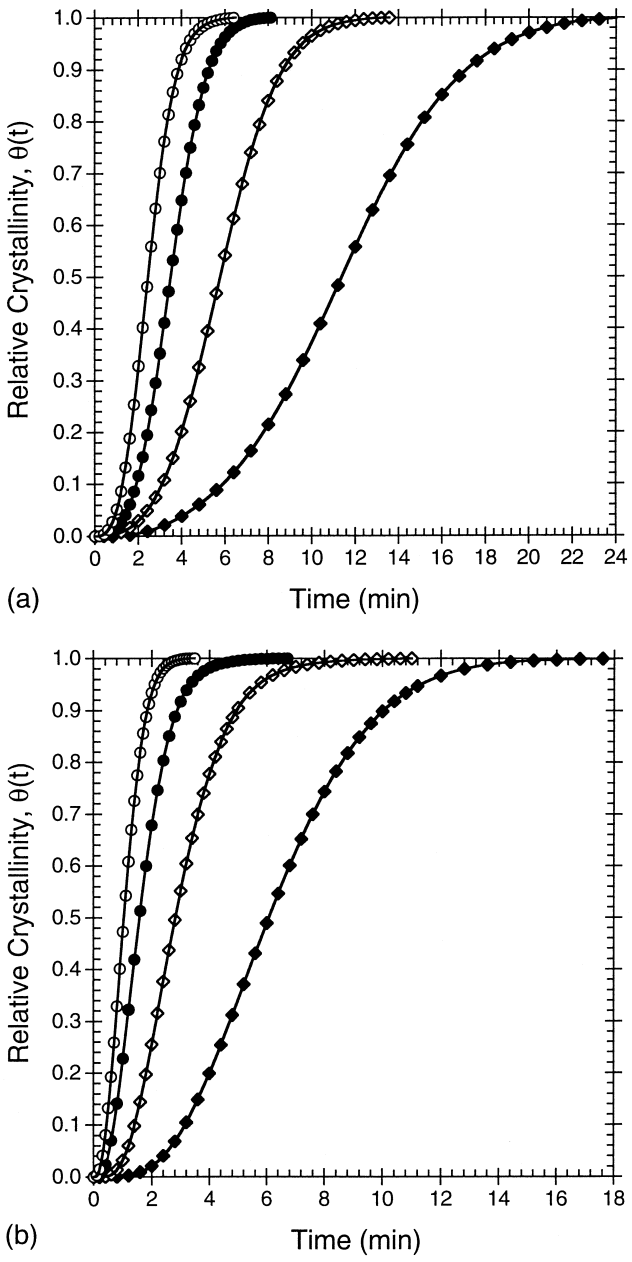

FIG. 1. Experimental relative crystallinity as a function of time of (a) sPP 1 and (b) sPP 3 for four crystallization temperatures: ○, 75°C; ●, 80°C; ◇, 85°C; ◆, 90°C.

MARCEL DEKKER, INC.
270 Madison Avenue, New York, New York 10016

TABLE 2

Overall Crystallization Kinetics Data for Syndiotactic Polypropylene Samples Based on the Avrami Model

	sPP 1							sPP 3						
T_c, °C	$t_{0.5}$, min	k_a^*, min^{-n}	n_a	k_a, min^{-n}	χ^2	n_a^{**}	k_a^{**}, min^{-n}	$t_{0.5}$, min	k_a^*, min^{-n}	n_a	k_a, min^{-n}	χ^2	n_a^{**}	k_a^{**}, min^{-n}
60.0	1.67	1.73×10^{-1}	2.71	1.75×10^{-1}	0.004	2.68	1.77×10^{-1}	—	—	—	—	—	—	—
62.5	1.70	1.63×10^{-1}	2.72	1.65×10^{-1}	0.007	2.74	1.64×10^{-1}	—	—	—	—	—	—	—
65.0	1.75	1.65×10^{-1}	2.56	1.66×10^{-1}	0.002	2.57	1.66×10^{-1}	—	—	—	—	—	—	—
67.5	1.83	1.48×10^{-1}	2.56	1.48×10^{-1}	0.016	2.59	1.46×10^{-1}	—	—	—	—	—	—	—
70.0	1.98	1.15×10^{-1}	2.63	1.14×10^{-1}	0.018	2.68	1.11×10^{-1}	—	—	—	—	—	—	—
72.5	2.18	8.71×10^{-2}	2.66	8.62×10^{-2}	0.018	2.73	8.22×10^{-2}	0.84	1.02	2.22	1.02	0.003	2.26	1.02
75.0	2.45	6.04×10^{-2}	2.72	5.95×10^{-2}	0.022	2.80	5.56×10^{-2}	1.04	6.38×10^{-1}	2.12	6.30×10^{-1}	0.004	2.15	6.30×10^{-1}
77.5	2.92	3.07×10^{-2}	2.91	3.06×10^{-2}	0.011	2.97	2.88×10^{-2}	1.18	4.96×10^{-1}	2.07	4.91×10^{-1}	0.009	2.11	4.89×10^{-1}
80.0	3.50	1.60×10^{-2}	3.01	1.59×10^{-2}	0.014	3.07	1.47×10^{-2}	1.58	2.69×10^{-1}	2.07	2.64×10^{-1}	0.051	2.17	2.53×10^{-1}
82.5	4.81	4.79×10^{-3}	3.17	4.75×10^{-3}	0.012	3.22	4.36×10^{-3}	1.96	1.58×10^{-1}	2.20	1.53×10^{-1}	0.123	2.34	1.40×10^{-1}
85.0	5.78	3.65×10^{-3}	2.99	3.64×10^{-3}	0.014	3.05	3.30×10^{-3}	2.82	6.38×10^{-2}	2.30	6.11×10^{-2}	0.154	2.48	5.14×10^{-2}
87.5	7.65	1.90×10^{-3}	2.90	1.90×10^{-3}	0.059	2.97	1.66×10^{-3}	3.85	3.20×10^{-2}	2.28	3.06×10^{-2}	0.226	2.49	2.35×10^{-2}
90.0	11.40	5.29×10^{-4}	2.95	5.32×10^{-4}	0.023	2.96	5.19×10^{-4}	6.08	7.09×10^{-3}	2.54	6.86×10^{-3}	0.076	2.67	5.48×10^{-3}
92.5	19.40	7.36×10^{-4}	2.31	7.10×10^{-4}	0.116	2.47	4.39×10^{-4}	9.71	1.80×10^{-3}	2.62	1.75×10^{-3}	0.062	2.74	1.33×10^{-3}
95.0	28.30	2.49×10^{-4}	2.37	2.50×10^{-4}	0.025	2.41	2.23×10^{-4}	17.23	1.88×10^{-4}	2.88	1.89×10^{-4}	0.002	2.87	1.98×10^{-4}

MARCEL DEKKER, INC. 270 Madison Avenue, New York, New York 10016

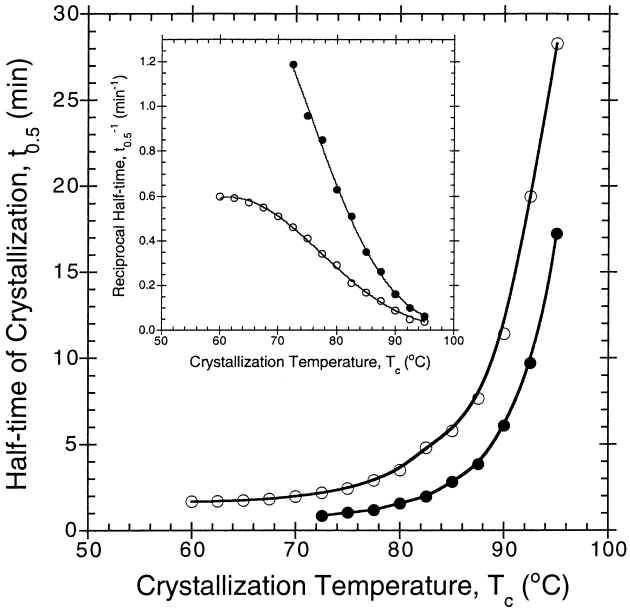

FIG. 2. Half-time of crystallization as a function of crystallization temperature, with the inset illustrating the reciprocal half-time as a function of crystallization temperature: ○, sPP 1; ●, sPP 3.

According to Fig. 2, it is evident that, for each sPP sample, the crystallization half-time $t_{0.5}$ increases with increasing crystallization temperature. The most fundamental representation of the bulk crystallization kinetics data is to plot the reciprocal of the half-time of crystallization $t_{0.5}^{-1}$ against the crystallization temperature. Such plots are illustrated in the inset of Fig. 2. If the crystallization half-time data can be collected with a minimal degree of error over the whole temperature range (i.e., $T_g < T_c < T_m^o$), the plot of $t_{0.5}^{-1}$ versus T_c should exhibit the typical bell-shaped curve, which can be described as a result of the nucleation control effect at low undercooling and of the diffusion control effect at high undercooling. Indeed, we have found a double bell-shaped curve on the plot of $t_{0.5}^{-1}$ versus T_c for the crystallization half-time data of sPP 1 [20]. An explanation of two maxima observed on the plot of $t_{0.5}^{-1}$ versus T_c is not known at this point and is a matter of an ongoing investigation. By comparing the plots of $t_{0.5}^{-1}$ versus T_c for both sPP samples shown in Fig. 2 with our earlier result [20], it is apparent that, within the temperature range of interest in this study (i.e., $60° < T_c < 95°C$), both samples crystallize in the region in which nucleation is the rate-determining factor. It is important to note that one of the maxima clearly seen on the plot of $t_{0.5}^{-1}$ versus T_c [20] for the whole range of temperatures for sPP 1 was at 60°C, corresponding to the maximum on the inset.

The result shown in Fig. 2 also suggests that sPP 3 crystallizes faster than sPP 1 even though its syndiotacticity level is a bit lower (cf. Table 1). This can be explained based on the facts that sPP 3 has a lower ethylene content (i.e., comonomer defects) in its molecular chains, and that sPP 3 consists of molecular chains of relatively lower molecular mass.

MARCEL DEKKER, INC.
270 Madison Avenue, New York, New York 10016

Application of the Avrami, Tobin, and Malkin Models

Instead of performing the data analysis in the traditional way, the experimental data were fitted iteratively to the respective macrokinetic models using a nonlinear multivariable regression program. As mentioned above, the goodness of the fit can be determined from the χ^2 values [18], in which the lower the value observed, the better the quality of the fit. The respective kinetics parameters were also provided by the program once the best fit was determined.

Isothermal Crystallization Kinetics Based on the Avrami Model

The analysis based on the Avrami model can be done by fitting the $\theta(t)$ function obtained for each crystallization temperature to Eq. 1. The Avrami exponent n_a, the crystallization rate constant k_a, and the χ^2 parameter, provided by the program, are summarized in Table 2. The exponent n_a for primary crystallization are found to range from 2.31 to 3.17 for sPP 1 (with the average value of 2.75 ± 0.2) and 2.07 to 2.88 for sPP 3 (with the average value of 2.33 ± 0.3). This may correspond to a two-dimensional growth with a combination of thermal and athermal nucleation (as a result of the fractional n_a values observed) [16]. Intuitively, the temperature dependence of the exponent n_a, within the nucleation control region (i.e., $60° < T_c < 95°C$), should be such that n_a decreases with decreasing temperature. This may be explained based on the fact that the number of athermal nuclei increases tremendously as the temperature decreases [19,21]. In other words, as the crystallization temperature decreases, the number of athermal nuclei that become stable at that temperature also increases, resulting in the nucleation mechanism becoming more instantaneous in time and causing the Avrami exponent n_a to decrease. Indeed, the decrease in n_a value with decreasing temperature can be observed from the results listed in Table 2, especially in the case of sPP 3.

According to Table 2, the crystallization rate constant k_a exhibits extreme sensitivity to the change in crystallization temperature, increasing with decreasing temperature. This is because sPP crystallizes faster at lower temperatures. This observation is only true when the temperature is in the range for which nucleation is the rate-determining factor (i.e., $60° < T_c < 95°C$ for sPP). A similar implication was addressed earlier based on the fact that the reciprocal half-time $t_{0.5}^{-1}$ also exhibits the same trend (cf. the inset of Fig. 2). Indeed, the rate constant k_a can be calculated directly from the reciprocal half-time $t_{0.5}^{-1}$ value, that is, $k_a^* = \ln 2 (t_{0.5}^{-1})^n$; the calculated rate constant values k_a^* are also summarized for comparison in Table 2. Obviously, there is good agreement between the rate constant obtained from the fit k_a and that obtained from the calculation k_a^*. In addition, at the same temperature, sPP 3 has a larger value of k_a than does sPP 1, suggesting that sPP 3 crystallizes more readily, as previously seen based on the $t_{0.5}^{-1}$ values.

Verification of the applicability and reliability of the fitting procedure in describing the isothermal crystallization data of sPP can be performed by comparison of the Avrami kinetics parameters n_a and k_a provided by the program to the ones obtained based on the traditional method [22] (listed in Table 2 as n_a^{**} and k_a^{**}, respectively). Apparently, extremely good agreement of the kinetics parameters obtained from the two different methods is obtained. This suggests that the fitting method can be used to analyze the isothermal crystallization data of sPP with a high level of confidence, and that it should also be applicable to other polymeric systems of similar molecular complexity.

MARCEL DEKKER, INC.
270 Madison Avenue, New York, New York 10016

Isothermal Crystallization Kinetics Based on the Tobin Model

The analysis based on the Tobin model can be performed by fitting the $\theta(t)$ function obtained for each crystallization temperature to Eq. 3. Table 3 summarizes the Tobin kinetics parameters n_t and k_t, as well as the χ^2 parameter. The Tobin exponents n_t for primary crystallization are found to range from 3.61 to 4.86 for sPP 1 and 3.29 to 4.44 for sPP 3. By comparison, it is apparent that at an arbitrary crystallization temperature, the Avrami exponent n_a is consistently lower in value than the Tobin exponent n_t. By taking the average of the difference between the two values, we are able to conclude, based on our experimental observation, that $n_t \approx n_a + 1.3$, which is in general accordance with observations by other researchers [14,15].

According to Table 3, the Tobin rate constant k_t clearly exhibits a similar trend to the Avrami rate constant k_a in that it is greater in its value at low crystallization temperature than that at high temperature. However, the change in the k_t value seems to be more sensitive to the change in the temperature than that exhibited by the Avrami rate constant k_a. According to Eq. 3, the Tobin rate constant k_t can also be calculated from the reciprocal half-time $t_{0.5}^{-1}$ value, that is, $k_t^* = (t_{0.5}^{-1})^n$. The calculated values k_t^* are also listed for comparison in Table 3. The discrepancy between the rate constant obtained from the fit k_t and that obtained from the calculation k_t^* of as much as 15% is found, as opposed to around a 3% difference in the k_a and k_a^* values. This suggests that the experimental data of sPP can be fitted to the Avrami model better than to the Tobin model. This can be confirmed based on the fact that the χ^2 parameters listed in Table 3 are much greater than those listed in Table 2.

TABLE 3

Overall Crystallization Kinetics Data for Syndiotactic Polypropylene Samples Based on the Tobin Model

	sPP 1					sPP 3				
T_c, °C	$t_{0.5}$, min	k_t^*, min^{-n}	n_t	k_t, min^{-n}	χ^2	$t_{0.5}$, min	k_t^*, min^{-n}	n_t	k_t, min^{-n}	χ^2
60.0	1.67	1.16×10^{-1}	4.19	1.35×10^{-1}	0.989	—	—	—	—	—
62.5	1.70	1.05×10^{-1}	4.25	1.21×10^{-1}	0.880	—	—	—	—	—
65.0	1.75	1.15×10^{-1}	3.86	1.31×10^{-1}	0.710	—	—	—	—	—
67.5	1.83	8.90×10^{-2}	4.00	1.01×10^{-1}	0.927	—	—	—	—	—
70.0	1.98	6.03×10^{-2}	4.11	6.80×10^{-2}	0.931	—	—	—	—	—
72.5	2.18	3.93×10^{-2}	4.15	4.38×10^{-2}	0.462	0.84	1.85	3.52	2.07	0.253
75.0	2.45	2.24×10^{-2}	4.24	2.48×10^{-2}	0.488	1.04	8.77×10^{-1}	3.36	9.69×10^{-1}	0.342
77.5	2.92	7.98×10^{-3}	4.51	9.02×10^{-3}	0.615	1.18	5.88×10^{-1}	3.29	6.52×10^{-1}	0.363
80.0	3.50	2.96×10^{-3}	4.65	3.33×10^{-3}	0.696	1.58	2.22×10^{-1}	3.30	2.42×10^{-1}	0.350
82.5	4.81	4.81×10^{-4}	4.86	5.40×10^{-4}	0.932	1.96	9.68×10^{-2}	3.47	1.04×10^{-1}	0.298
85.0	5.78	3.03×10^{-4}	4.62	3.42×10^{-4}	0.790	2.82	2.35×10^{-2}	3.62	2.49×10^{-2}	0.223
87.5	7.65	1.06×10^{-4}	4.50	1.20×10^{-4}	1.055	3.85	8.02×10^{-3}	3.58	8.49×10^{-3}	0.153
90.0	11.40	1.51×10^{-5}	4.56	1.73×10^{-5}	1.419	6.08	7.80×10^{-4}	3.96	8.45×10^{-4}	0.326
92.5	19.40	2.27×10^{-5}	3.61	2.43×10^{-5}	0.518	9.71	9.50×10^{-5}	4.07	1.04×10^{-4}	0.293
95.0	28.30	3.71×10^{-6}	3.74	4.21×10^{-6}	0.965	17.23	3.25×10^{-6}	4.44	3.71×10^{-6}	0.779

MARCEL DEKKER, INC.
270 Madison Avenue, New York, New York 10016

Isothermal Crystallization Kinetics Based on the Malkin Model

The analysis based on the Malkin model can be carried out by fitting the $\theta(t)$ function obtained for each crystallization temperature to Eq. 4. The kinetics parameters characteristic of the Malkin model C_0 and C_1, as well as the χ^2 parameter, are listed in Table 4. The C_0 parameter is found to range from 25.11 to 107.27 for s-PP 1 and from 15.43 to 66.91 for sPP 3. Fundamentally, the C_0 parameter, which relates directly to the n_a value through Eq. 5, should exhibit a similar temperature dependence to that of the Avrami exponent n_a. Indeed, such a trend can be deduced from the results listed in Table 4, especially in the case of sPP 3. According to Table 4, the Malkin rate constant C_1 also exhibits a temperature dependence in a similar fashion as the crystallization rate constants characteristic of both the Avrami and Tobin models.

Unlike the Avrami and the Tobin models, there is no direct analytical procedure for the determination of the Malkin kinetics parameters. Without the direct-fitting method utilized in this study, the Malkin kinetics parameters C_0 and C_1 can only be estimated from the Avrami kinetics parameters n_a and k_a through the relationships set forth in Eqs. 5 and 6. The estimated Malkin kinetics parameters are also listed in Table 4, in which they are denoted C_0^* and C_1^*, respectively. Evidently, the estimated rate constant C_1^* is found to be in good agreement with that obtained from the direct-fitting method C_1. Like the other two rate constants, the Malkin rate constant C_1 can also be calculated directly from the reciprocal half-time $t_{0.5}^{-1}$ value, that is, $C_1 = \ln(4^n - 2)(t_{0.5}^{-1})$. Although not listed in Table 4, the C_1 values calculated from the $t_{0.5}^{-1}$ values are found to be almost identical to the estimated Malkin crystallization rate values C_1^*.

TABLE 4

Overall Crystallization Kinetics Data for Syndiotactic Polypropylene Samples Based on the Malkin Model

	sPP 1					sPP 3				
T_c, °C	C_0	C_1, min^{-1}	χ^2	C_0^*	C_1^*, min^{-1}	C_0	C_1, min^{-1}	χ^2	C_0^*	C_1^*, min^{-1}
60.0	49.90	2.37	0.066	38.74	2.26	—	—	—	—	—
62.5	51.56	2.34	0.055	39.65	2.23	—	—	—	—	—
65.0	38.70	2.11	0.064	31.01	2.04	—	—	—	—	—
67.5	38.80	2.02	0.072	30.63	1.94	—	—	—	—	—
70.0	44.44	1.93	0.088	34.47	1.84	—	—	—	—	—
72.5	46.85	1.77	0.052	36.04	1.69	20.98	3.69	0.033	17.79	3.66
75.0	52.18	1.62	0.064	39.61	1.53	17.05	2.79	0.049	14.87	2.81
77.5	70.62	1.46	0.047	52.36	1.38	15.43	2.39	0.067	13.61	2.43
80.0	83.04	1.27	0.057	60.60	1.19	15.64	1.78	0.140	13.67	1.80
82.5	107.27	0.97	0.104	76.65	0.91	20.35	1.55	0.242	17.05	1.53
85.0	80.65	0.76	0.048	59.18	0.72	25.06	1.14	0.261	20.35	1.11
87.5	69.58	0.56	0.026	51.65	0.53	24.25	0.83	0.322	19.69	0.81
90.0	74.95	0.38	0.057	55.65	0.36	38.35	0.60	0.167	29.77	0.57
92.5	25.11	0.17	0.235	20.57	0.16	44.12	0.39	0.126	33.80	0.37
95.0	27.91	0.12	0.079	22.83	0.12	66.91	0.25	0.059	50.52	0.23

MARCEL DEKKER, INC.
270 Madison Avenue, New York, New York 10016

Comparison Among the Different Isothermal Macrokinetic Models

The quality of the model in describing the experimental isothermal measurements is numerically represented by the χ^2 parameter, in which the lower the value is, the better will be the quality of the fit. By comparing the values of the χ^2 parameter listed in Tables 2 to 4, we can conclude that only the Avrami and the Malkin models can be used to describe the primary process of the isothermal evolution of crystallinity in sPP well. This is accented by visual verification illustrated in Fig. 3, in which the experimental time-dependent relative crystallinity functions $\theta(t)$ collected at two crystallization temperatures (75°C and 85°C) are plotted against the best-fitted curves provided by the program. Clearly, the goodness of the fitted curves according to the Avrami and the Malkin models (shown in Fig. 3 as solid and dashed lines, respectively) is of greater quality than the fitted curve according to the Tobin model (shown in Fig. 3 as dotted lines). As a result, the Tobin model will not be considered further. In addition, the Avrami model seems to give a better prediction than the Malkin model in the early stage of crystallization [ca. $0.15 \leq \theta(t)$], whereas, the Malkin model seemingly provides a better fit at the later stage of crystallization [ca. $\theta(t) \geq 0.85$].

Application of the Simultaneous Avrami Model

Applicability of the Avrami and the Malkin models for describing the experimental isothermal crystallization measurements of sPP was verified above. Due to the fact that the Avrami kinetics parameters n_a and k_a are very well defined according to Table 5 and that those of the Malkin model, C_0 and C_1, are not entirely understood (but they are worth looking into, and it is a subject of further investigation), the applicability of the Avrami model for the prediction of the isothermal crystallization will be further discussed.

One of the serious discrepancies that questions the applicability of the Avrami model is that, in most cases, the analysis of the experimental data based on the Avrami equation leads to fractional values of the Avrami exponent n_a (cf. Table 2). The nonintegral observations of the Avrami exponent n_a may be explained as follows:

1. The discrepancies in the assumptions used in the derivation of the model.
2. Inaccuracy in the determination of the onset of the crystallization process (if the onset is set prematurely, the value of the Avrami exponent n_a will be greater than the actual value, while that of the rate constant k_a will be smaller).
3. Changes in the nucleation rate N and growth rate G during the crystallization process (if the values decrease, the value of the Avrami exponent n_a will also decrease).
4. Changes in the morphology during the crystallization process (i.e., sheaflike to spherulitic). This may also include the occurrence of the secondary crystallization in which internal changes in the crystal morphology are experimentally observed [1–3].

In addition to the above explanations, the fractional value of the Avrami exponent n_a may also be elucidated based on the hypothesis that crystalline aggregates grow concurrently from both instantaneous and sporadic nuclei (as opposed to growing from only one type of nuclei, assumed in the original theory), as mentioned above. Indeed, observation made on an optical microscope confirms that, for a given crystallization temperature, a certain number of nuclei are activated instantaneously, while others are activated sporadically. It should be noted that the observation is valid within the crystallization tem-

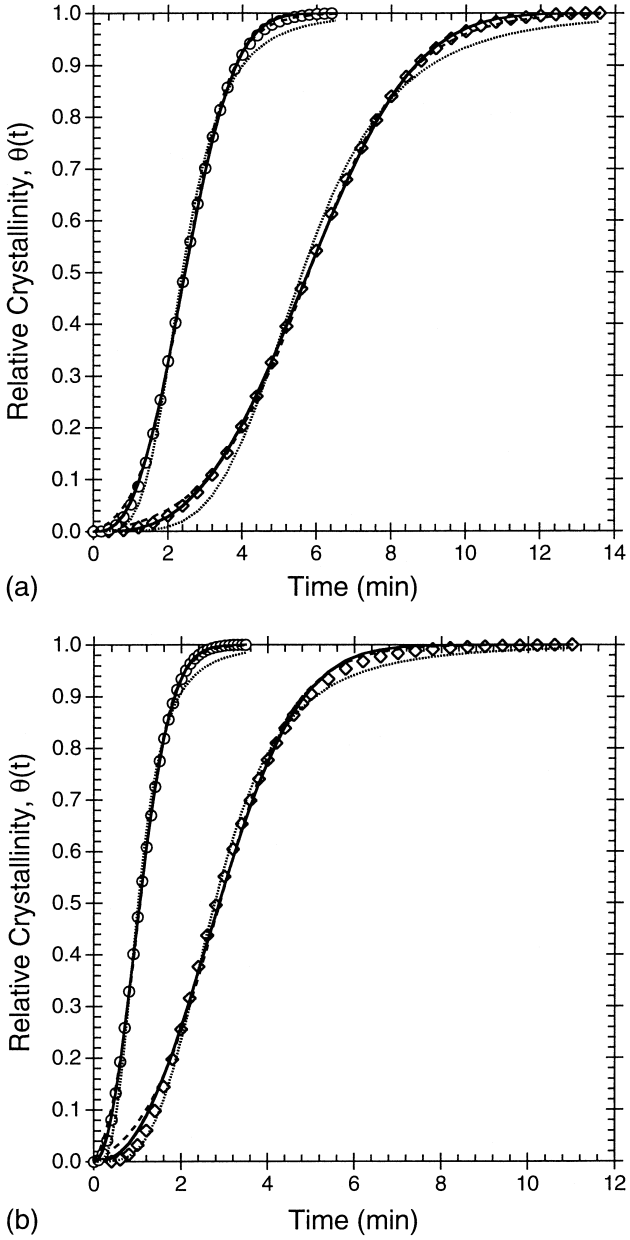

FIG. 3. Relative crystallinity as a function of time of (a) sPP 1 and (b) sPP 3 for two crystallization temperatures: ○, 75°C; ◇, 85°C. The experimental data, shown as points, were fitted to the nonlinear multivariable regression program, for which the best fits according to the Avrami, the Tobin, and the Malkin macrokinetic models are shown as the solid, dotted, and dashed lines, respectively.

MARCEL DEKKER, INC.
270 Madison Avenue, New York, New York 10016

TABLE 5

Theoretical Description of the Avrami Isothermal Crystallization Rate Constant k_a for Different Types of Morphology and Transient Nucleation

		Isothermal crystallization rate constant[a]	
Crystal morphology	Morphological dimensionality, n	Instantaneous nucleation k_{ai}, min^{-n}	Sporadic nucleation k_{as}, $\text{min}^{-(n+1)}$
Rod	1	N_0GA	$1/2 \cdot NGA$
Disk	2	πN_0G^2D	$\pi/3 \cdot NG^2D$
Sphere	3	$4\pi/3 \cdot N_0G^3$	$\pi/3 \cdot NG^3$

[a]A is constant area, D is the disk thickness, G is the linear crystal growth rate, N_0 is the concentration of predetermined nuclei, and N is the nucleation rate.

perature range 60°C to 95°C. Based on this experimental observation, the original Avrami equation can be modified to account for both types of transient nucleation. The modified equation, called the simultaneous Avrami model, can be written as

$$\theta(t) = 1 - \exp(-k_{ai}t^n - k_{as}t^{n+1}) \tag{7}$$

where $\theta(t)$ denotes the relative crystallinity as a function of time, and n is the morphological dimensionality, which ranges from 1 to 3 (i.e., rod, disk, and sphere). In Eq. 7, k_{ai} and k_{as} are the crystallization rate constants specific for instantaneous and sporadic nucleation, respectively (cf. Table 5). It should be noted that a similar equation was first used to explain the fractional values of the Avrami exponent n_a by Banks et al. [23], but they concluded then that the equation was not satisfactory in accounting for the occurrence of the fractional values of n_a.

Analysis of the isothermal crystallization data based on the simultaneous Avrami model can be done very readily by fitting the $\theta(t)$ function to Eq. 7 using the nonlinear multivariable regression program, as opposed to the trial-and-error method utilized by Banks et al. [23]. According to the Avrami analysis (cf. Table 2), n_a ranges mainly between 2 and 3, suggesting two-dimensional growth geometry (perhaps due to a truncation of the spherulitic structure). Thus, we chose a value of n in Eq. 7 equal to 2. The crystallization rate constant for the instantaneous nucleation process k_{ai}, the crystallization rate constant for the sporadic nucleation process k_{as}, and the χ^2 parameter, which were provided by the best fit according to the program, are summarized in Table 6. Clearly, the values of both rate constants exhibit a temperature dependence in the same manner as do the rate constants characteristic of the three other models.

Comparison of the χ^2 parameters given in Table 6 with those listed in Tables 2 to 4 suggests that the quality of the simultaneous Avrami model in describing the isothermal crystallization data is comparable to that of the Avrami model and is a little better than that of the Malkin model. This further suggests that applicability of the model in describing isothermal crystallization in sPP (and, perhaps, other polymers) is satisfactory. Even though the reasons for the rejection of the similar equation given by Banks et al. [23]

TABLE 6

Overall Crystallization Kinetics Data for Syndiotactic Polypropylene Samples Based on the Simultaneous Avrami Model

	sPP 1			sPP 3		
T_c °C	k_{ai}, min^{-2}	k_{as}, min^{-3}	χ^2	k_{ai}, min^{-2}	k_{as}, min^{-3}	χ^2
60.0	9.76×10^{-2}	1.06×10^{-1}	0.001	—	—	—
62.5	9.02×10^{-2}	1.04×10^{-1}	0.017	—	—	—
65.0	7.20×10^{-2}	7.31×10^{-2}	0.016	—	—	—
67.5	6.43×10^{-2}	6.27×10^{-2}	0.045	—	—	—
70.0	6.25×10^{-2}	5.65×10^{-2}	0.052	—	—	—
72.5	4.66×10^{-2}	4.41×10^{-2}	0.039	7.75×10^{-1}	2.34×10^{-1}	0.011
75.0	2.93×10^{-2}	3.40×10^{-2}	0.044	5.68×10^{-1}	6.03×10^{-2}	0.009
77.5	6.36×10^{-3}	2.55×10^{-2}	0.015	4.72×10^{-1}	2.11×10^{-2}	0.014
80.0	4.84×10^{-3}	1.63×10^{-2}	0.013	2.62×10^{-1}	1.41×10^{-2}	0.063
82.5	1.27×10^{-3}	7.21×10^{-3}	0.003	1.46×10^{-1}	8.01×10^{-3}	0.176
85.0	1.09×10^{-3}	3.57×10^{-3}	0.015	6.04×10^{-2}	6.95×10^{-3}	0.228
87.5	9.10×10^{-4}	1.40×10^{-3}	0.064	3.35×10^{-2}	2.87×10^{-3}	0.310
90.0	5.50×10^{-4}	4.45×10^{-4}	0.021	8.18×10^{-3}	1.60×10^{-3}	0.132
92.5	2.80×10^{-4}	2.56×10^{-5}	0.188	2.57×10^{-3}	4.62×10^{-4}	0.106
95.0	5.63×10^{-5}	1.09×10^{-5}	0.045	2.68×10^{-4}	1.20×10^{-4}	0.000

were valid, we suggest that the simultaneous Avrami model may be more suitable than the original Avrami model in describing overall isothermal crystallization in polymers.

Prediction of Isothermal Crystallization Kinetics

The crystallization kinetics parameters (cf. Tables 2, 4, and 6) determined from limited experimental isothermal measurements can be used to predict the time-dependent relative evolution of the crystallinity $\theta(t)$ at other temperatures. The prediction can be carried out by virtue of the following facts:

1. The crystallization rate parameters (i.e., $t_{0.5}^{-1}$, k_a, C_1, k_{ai}, or k_{as}) determined based on different macrokinetic models exhibit a finite temperature dependence.
2. The crystallization rate parameters relate, in one way or another, to the primary nucleation rate N and/or the subsequent crystal growth rate G, especially the crystallization rate parameters of the Avrami and the simultaneous Avrami models (cf. Table 5).
3. The temperature dependence of the primary nucleation rate N and the subsequent crystal growth rate G are well defined in the literature [24–26]. Even though the temperature dependence of the parameters N and G are different [i.e., $N \propto (\Delta T)^{-2}$ and $G \propto (\Delta T)^{-1}$, respectively], the crystallization rate parameters have often been taken as temperature dependence similar to that of the subsequent crystal growth rate G, written in the context of the original Lauritzen and Hoffman secondary nucleation theory (LH theory) [25,26], which can be expressed as

$$\Psi(T) = \Psi_0 \exp\left\{-\frac{\Theta}{R[T_c - (T_g - \delta)]} - \frac{K}{T_c(\Delta T)f}\right\} \quad (8)$$

where $\Psi(T)$ and Ψ_0 are the respective crystallization rate function (i.e., $t_{0.5}^{-1}$, k_a, C_1, k_{ai}, or k_{as}) and the respective preexponential parameter [i.e., $(t_{0.5}^{-1})_0$, k_{a0}, C_{10}, k_{ai0}, or k_{as0}), respectively. Θ is a parameter related to the activation energy characterizing the molecular diffusion across the melt/crystal interface, while (is a parameter related to the secondary nucleation. T_c is the crystallization temperature; T_g is the glass transition temperature (ca. −6.1°C [22]); δ is a WLF parameter that indicates the cessation of molecular motion and is often taken to be either about 30 K or about 50 K; R is the universal gas constant; ΔT is the degree of undercooling, that is, $\Delta T = T_m^o - T_c$, where T_m^o is taken to be 168.7°C [22]; and finally, f is a factor used to correct for the temperature dependence of the heat of fusion, that is, $2T_c/(T_c + T_m^o)$.

It should be noted that a critical analysis of the linear growth rate G of sPP in the context of the LH theory can be found in a publication by the same authors [27]. The analysis suggested an unmistakable transition from regime II to regime III at the crystallization temperature T_c of 110°C. Since, in this study, the temperature range of interest apparently falls in regime III, the complication that arises from change of the secondary nucleation exponent (i.e., K) due to the change in regimes can be ignored as long as the temperature range of interest is lower than 110°C.

The temperature-dependent crystallization rate function $\Psi(T)$ can be easily determined by fitting the respective crystallization rate parameters (i.e., $t_{0.5}^{-1}$, k_a, C_1, k_{ai}, or k_{as}) collected at various crystallization temperatures to Eq. 8 using the same nonlinear multivariable regression program. As soon as the $\Psi(T)$ function is determined, values of the respective rate parameters at other temperatures can then be estimated. By substitution of the calculated rate constant at a temperature of interest into the appropriate macrokinetic model, the time-dependent relative crystallinity $\theta(t)$ at that temperature can readily be predicted if the appropriate value of time exponent (i.e., n_a or C_0) is assumed (due to the lack of finite relationship of these parameters with the temperature, usually assumed to be the arithmetic mean of the experimental observations). The discrepancy that may arise from the uncertainty of the time exponent assumed may be remedied using the simultaneous Avrami model since it does not involve the selection of the dimensionality parameter (provided that changes in crystal morphology do not occur over the temperature range of interest).

To obtain the best possible fits for the rate parameters with Eq. 8, the δ value was chosen to be either 30 K or 50 K, while those of T_g and T_m^o are fixed, as noted above. In doing so, the only unknown parameters provided by the program, once the fit was determined, are Ψ_0, Θ, and K. Plots of the rate parameters of interest (i.e., $t_{0.5}^{-1}$, k_a, C_1, k_{ai}, and k_{as}) and their corresponding best fit for both samples are illustrated in Fig. 4, whereas the values of δ, Ψ_0, Θ, and K, as well as the χ^2 parameter as a result of the best fits, are summarized in Table 7. Judging from the χ^2 parameters listed in Table 7, the goodness of the fits of these rate parameters with Eq. 8 is very satisfactory. Now that all of the parameters in Eq. 8 are known, the rate parameters of interest at other temperatures can be estimated.

Using the kinetics parameters summarized in Table 7, the prediction of the time-dependent relative crystallinity functions $\theta(t)$ for $T_c = 85$°C and 90°C for both of the sPP samples studied can be demonstrated as illustrated in Fig. 5. In general, the quality of

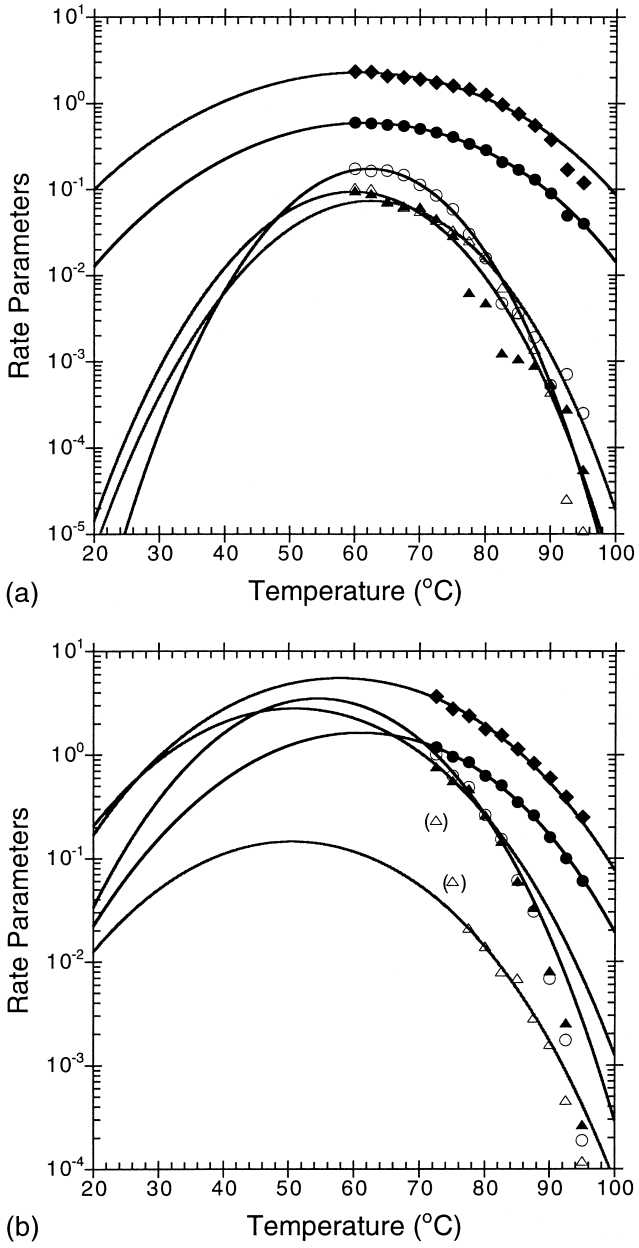

FIG. 4. The best-fitted curves of various crystallization rate parameters of (a) sPP1 and (b) sPP3 to Eq. 8: ●, $t_{0.5}^{-1}$; ○, k_a; ◆, C_1; ▲, k_{ai}; △, k_{as}.

TABLE 7

Fitting Parameters, as Provided by the Program, for the Best Possible Fits of the Respective Rate Parameters to Equation 8

Ψ	δ, K	Ψ_0	Θ, cal·mol^{-1}	K, K^2	χ^2
sPP 1					
$t_{0.5}^{-1}$, min^{-1}	50	3.31×10^{13}	2617	6.32×10^5	0.0006
k_a, min$^{-2.75}$	50	9.09×10^{42}	8476	1.99×10^6	0.0002
C_1, min^{-1}	50	1.06×10^{12}	2175	5.43×10^5	0.0861
k_{ai}, min^{-2}	50	7.23×10^{33}	6301	1.65×10^6	0.0004
k_{as}, min^{-3}	50	4.99×10^{30}	6222	1.44×10^6	n/a
sPP 3					
$t_{0.5}^{-1}$, min^{-1}	50	1.39×10^{16}	2982	7.39×10^5	0.0035
k_a, min$^{-2.33}$	50	9.26×10^{25}	3910	1.30×10^6	0.0064
C_1, min^{-1}	30	8.09×10^{12}	1500	6.28×10^5	0.0977
k_{ai}, min^{-2}	50	5.30×10^{18}	2500	9.79×10^5	0.0091
k_{as}, min^{-3}	50	6.12×10^{16}	2380	9.49×10^5	n/a

the predicted $\theta(t)$ functions is rather disappointing. The deviation of the predicted curve at an arbitrary crystallization temperature may arise from the deviation of the predicted value of the corresponding crystallization rate parameter from the actual value at that temperature. In the Avrami and the Malkin models, another problem exists as a result of the supposition made on the value of the respective time exponent (i.e., n_a or C_0), which has to be fixed (e.g., the average value of the experimental results) when the prediction is carried out. It is fair to state, however, that prediction made for some other crystallization temperatures, for which the deviation of the estimated values of the corresponding rate parameter (i.e., $t_{0.5}^{-1}$, k_a, C_1, k_{ai}, and k_{as}) from the experimentally observed values is minimal, may be more accurate than what has been demonstrated here.

CONCLUSIONS

A nonlinear multivariable regression program was used to fit the isothermal crystallization measurements obtained from the DSC to four macrokinetic models (Avrami, Tobin, Malkin, and simultaneous Avrami) and was found to give reliable kinetics results. Judging from the quality of the fit, only the Avrami, Malkin, and simultaneous Avrami models were found to describe the time dependence of the relative crystallinity well, resulting in the rejection of the Tobin model in describing the isothermal crystallization of sPP.

The Avrami exponent was found to be in the approximate range of 2 to 3, suggesting two-dimensional growth from a combination of thermal and athermal nuclei (i.e., instantaneous and sporadic nucleation). All of the crystallization rate parameters (i.e., $t_{0.5}^{-1}$, k_a, k_t, C_1, k_{ai}, and k_{as}) are found to be very sensitive to changes in the crystallization temperature. Within the crystallization temperature range studied (i.e., $60° < T_c < 95°C$), the values of the rate parameters were all found to increase with decreasing temperature due to the fact that sPP crystallizes faster at lower temperature than at the higher tempera-

MARCEL DEKKER, INC.
270 Madison Avenue, New York, New York 10016

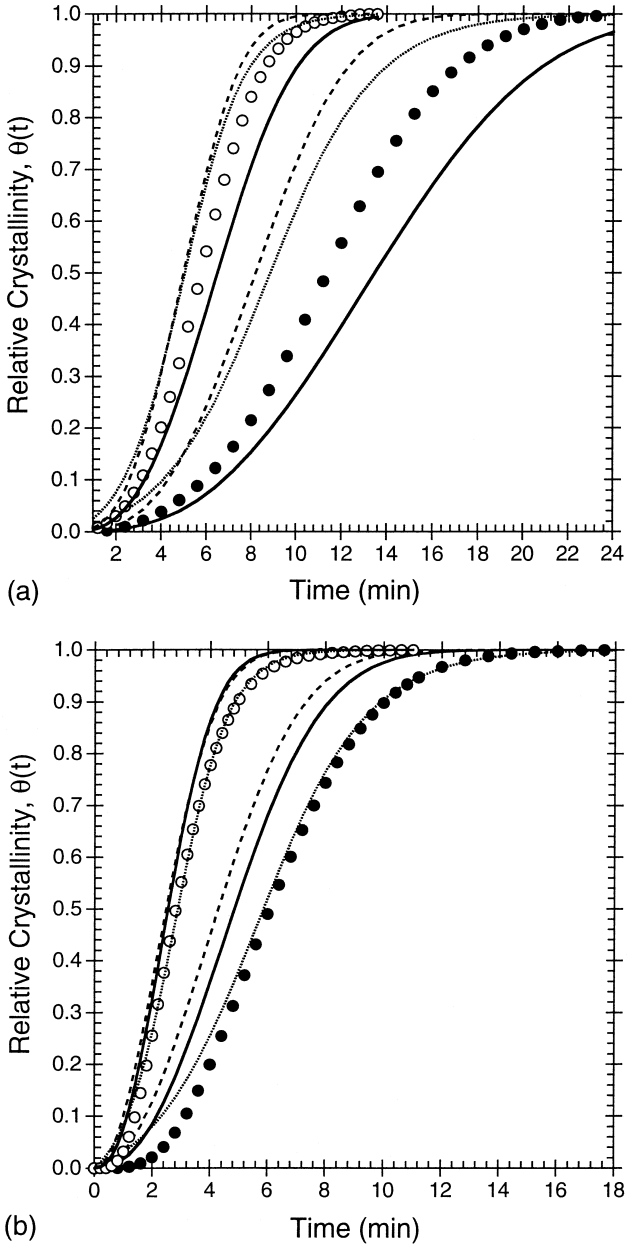

FIG. 5. Relative crystallinity as a function of time of (a) sPP 1 and (b) sPP 3 for two crystallization temperatures: ○, 85°C; ●, 90°C. The experimental data, shown as points, are plotted along with the predicted curves using the Avrami, the Malkin, and the simultaneous Avrami macrokinetics models (shown as the solid, dotted, and dashed lines, respectively).

MARCEL DEKKER, INC.
270 Madison Avenue, New York, New York 10016

ture. Comparison with earlier results [20] suggested that the range of temperature in this study falls in the region in which nucleation is the rate-determining factor. In addition, at the same temperature, sPP 3 was found to crystallize faster than sPP 1, even though its syndiotacticity level is a bit lower. The explanation was given based on the facts that the sPP 3 possesses a lower level of ethylene comonomer defects, and that sPP 3 consists of molecular chains of relatively lower molecular mass.

It was shown that all of the crystallization rate parameters (i.e., $t_{0.5}^{-1}$, k_a, k_t, C_1, k_{ai}, and k_{as}) have a definable relationship with crystallization temperature (or degree of undercooling), making it possible to estimate values of the corresponding rate parameters at other temperatures and hence possible predictions of the isothermal crystallization at those temperatures.

ACKNOWLEDGMENTS

We would like to thank Dr. Joseph Schardl of Fina Oil and Chemical Company in Dallas, Texas, for supplying the sPP samples and Dr. Roger A. Phillips and his coworkers of Montell USA, Incorporated, in Elkton, Maryland, for performing sample characterizations.

REFERENCES

1. H. D. Keith and F. J. Padden, *J. Appl. Phys*., *35*, 1270 (1964).
2. H. D. Keith and F. J. Padden, *J. Appl. Phys*., *35*, 1286 (1964).
3. R. Verma, H. Marand, and B. Hsiao, *Macromolecules*, *29*, 7767 (1996).
4. A. N. Kolmogoroff, *Izvestiya Akad. Nauk USSR, Ser. Math*., *1*, 355 (1937).
5. W. A. Johnson and K. F. Mehl, *Trans. Am. Inst. Mining Met. Eng*., *135*, 416 (1939).
6. M. Avrami, *J. Chem. Phys*., *7*, 1103 (1939).
7. M. Avrami, *J. Chem. Phys*., *8*, 212 (1940).
8. M. Avrami, *J. Chem. Phys*., *9*, 177 (1941).
9. U. R. Evans, *Trans. Faraday Soc*., *41*, 365 (1945).
10. M. C. Tobin, *J. Polym. Sci., Polym. Phys*., *12*, 399 (1974).
11. M. C. Tobin, *J. Polym. Sci., Polym. Phys*., *14*, 2253 (1976).
12. M. C. Tobin, *J. Polym. Sci., Polym. Phys*., *15*, 2269 (1977).
13. A. Ya. Malkin, V. P. Beghishev, I. A. Keapin, and S. A. Bolgov, *Polym. Eng. Sci*., *24*(18), 1396 (1984).
14. K. Ravindranath and J. P. Jog, *J. Appl. Polym. Sci*., *49*, 1395 (1993).
15. J. J. C. Cruz-Pinto, J. A. Martins, and M. J. Oliveira, *Colloid Polym. Sci*., *272*, 1 (1994).
16. B. Wunderlich, in *Macromolecular Physics*, Vol. 2, Academic, New York, 1976, pp. 132–147.
17. J. Rabesiaka and A. J. Kovacs, *J. Appl. Phys*., *32*(11), 2314 (1961).
18. E. Kreyszig, in *Advanced Engineering Mathematics*, 7th ed., John Wiley and Sons, New York, 1993, pp. 1255–1257.
19. P. Supaphol and J. E. Spruiell, *J. Appl. Polym. Sci*., in press.
20. P. Supaphol, J. J. Hwu, P. J. Phillips, and J. E. Spruiell, *Proc. 55th Annual Tech. Conf.* (*ANTEC*), 1759 (1997).
21. H. Janeschitz-Kriegl, E. Ratajski, and H. Wippel, *Colloid Polym. Sci*., *277*, 217 (1999).
22. P. Supaphol and J. E. Spruiell, *J. Appl. Polym. Sci*., in press.
23. W. Banks, A. Sharples, and J. N. Hay, *J. Polym. Sci*., *A2*, 4059 (1964).
24. B. Wunderlich, in *Macromolecular Physics*, Vol. 2, Academic, New York, 1976, chap. 5.

25. J. D. Hoffman, G. T. Davis, and J. I. Lauritzen, Jr., in *Treatise on Solid State Chemistry*, Vol. 3 (N. B. Hannay, Ed.), Plenum, New York, 1976, chap. 7.
26. J. D. Hoffman and R. L. Miller, *Polymer*, *38*, 3151 (1997).
27. P. Supaphol and J. E. Spruiell, *Polymer*, *41*(3), 1205 (2000).

Received March 25, 1999
Revised May 28, 1999
Accepted May 31, 1999